

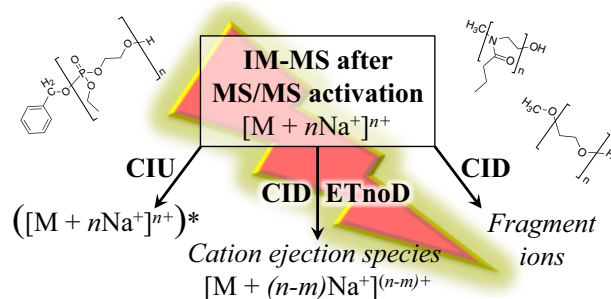
Gas-Phase Dynamics of Collision Induced Unfolding, Collision Induced Dissociation, and Electron Transfer Dissociation-Activated Polymer Ions

Jean R. N. Halder,¹ Philippe Massonnet,¹ Johann Far,¹ Victor R. de la Rosa,² Philippe Lecomte,³ Richard Hoogenboom,² Christine Jérôme,³ Edwin De Pauw¹

¹Mass Spectrometry Laboratory, MolSys Research unit, Quartier Agora, University of Liège, Allée du Six Aout 11, B-4000, Liège, Belgium

²Supramolecular Chemistry Group, Centre of Macromolecular Chemistry (CMAc), Department of Organic and Macromolecular Chemistry, Ghent University, Krijgslaan 281 S4, B-9000, Ghent, Belgium

³Center for Education and Research on Macromolecules, CESAM Research Unit, Quartier Agora, University of Liège, Allée du Six Aout 13, B-4000, Liège, Belgium



Abstract. Polymer characterizations are often performed using mass spectrometry (MS). Aside from MS and different tandem MS (MS/MS) techniques, ion mobility–mass spectrometry (IM-MS) has been recently added to the inventory of characterization technique. However, only few studies have focused on the reproducibility and robustness of polymer IM-MS analyses. Here, we perform collisional and electron-mediated activation of polymer ions before measuring IM drift times,

collision cross-sections (CCS), or reduced ion mobilities (K_0). The resulting IM behavior of different activated product ions is then compared to non-activated native intact polymer ions. First, we analyzed collision induced unfolding (CIU) of precursor ions to test the robustness of polymer ion shapes. Then, we focused on fragmentation product ions to test for shape retentions from the precursor ions: cation ejection species (CES) and product ions with m/z and charge state values identical to native intact polymer ions. The CES species are formed using both collision induced dissociation (CID) and electron transfer dissociation (ETD, formally ETnOD) experiments. Only small drift time, CCS, or K_0 deviations between the activated/formed ions are observed compared to the native intact polymer ions. The polymer ion shapes seem to depend solely on their mass and charge state. The experiments were performed on three synthetic homopolymers: poly(ethoxy phosphate) (PEtP), poly(2-*n*-propyl-2-oxazoline) (P*n*-PrOx), and poly(ethylene oxide) (PEO). These results confirm the robustness of polymer ion CCSs for IM calibration, especially singly charged polymer ions. The results are also discussed in the context of polymer analyses, CCS predictions, and probing ion–drift gas interaction potentials.

Keywords: Collision induced unfolding, CIU, Collision induced dissociation, CID, Electron transfer dissociation, ETD, Synthetic polymers, Ion mobility calibration

Received: 4 October 2018/Revised: 24 November 2018/Accepted: 24 November 2018/Published Online: 6 December 2018

Electronic supplementary material The online version of this article (<https://doi.org/10.1007/s13361-018-2115-7>) contains supplementary material, which is available to authorized users.

Correspondence to: Jean Halder; e-mail: jean.halder@uliege.be

Introduction

Complex tandem mass spectrometry (MS/MS) polymer characterizations can be performed using different gas-phase activation techniques. Collision induced dissociation (CID), electron transfer dissociation (ETD), and electron

capture dissociation (ECD) are among the most commonly used MS/MS techniques for polymer structure elucidation [1–25]. The polymer chain end functions, the sequence of copolymers, MS/MS degradation and depolymerization mechanisms, as well as contamination analyses in complex polymer samples could thus be studied. More recently, coupling of MS techniques such as ion mobility–mass spectrometry (IM-MS) further enabled the analysis of complex samples [26–33]. The polymers could be differentiated according to their size and shape. The use of MS/MS with IM-MS experiments enhances polymer characterizations even further [5, 26, 30–36].

The scope of this study is to analyze shape variations of activated polymer ions and their product ions compared to the non-activated native intact precursor ions with identical m/z and charge states using IM-MS. This paper constitutes both a robustness study of polymer ion shapes in the gas phase as well as an experimental assessment of the shape evolution of polymer ions after activation. Both CID and ETD experiments are performed before the IM analysis. First, we analyze the drift times (and collision cross-sections; CCS) of collisionally activated intact poly(ethoxy phosphate) (PEtP) polymer ions through so-called collision induced unfolding experiments (CIU). Then we analyze the IM-measured shapes of the species having ejected one or more cations from their precursor ions using CID and (charge reduction) ETD, formally ETnoD (electron transfer no dissociation). Finally, the shapes of fragment ions, resulting in mass-to-charge (m/z) ratios of depolymerized polymer ions, are compared to the shapes of their native intact counterparts. Additionally to PEtP, this analysis is also performed on poly(2-*n*-propyl-2-oxazoline) (*Pn*-PrOx) and poly(ethylene oxide) (PEO).

Materials and Methods

Polymers

Poly(ethoxy phosphate) or poly(2-ethoxy-1,3,2-dioxaphospholane 2-oxide) (PEtP), poly(2-*n*-propyl-2-oxazoline) (*Pn*-PrOx), and poly(ethylene oxide) (PEO) polymers (see Figure S11) were dissolved in pure methanol and spiked with Na⁺ cations (NaCl salt) to yield solution concentrations of around 10^{-6} to $5 \cdot 10^{-6}$ M in both polymers and sodium. The PEtP sample—synthesized as reported in [34]—was 3000 g/mol and the *Pn*-PrOx sample—synthesized as reported in [37]—was 2600 g/mol (see Figure S115). PEO 750 and 2000 g/mol samples were bought from Aldrich (St. Louis, USA).

Ion Mobility–Mass Spectrometry (IM-MS)

The polymer samples were infused at a flow rate of 4 $\mu\text{L}/\text{min}$, using a syringe pump and a 250- μL Thermo Scientific syringe, into a Synapt G2 HDMS (Waters, Manchester, UK) or a timsTOF (Bruker, Germany) ion mobility–mass spectrometer.

Both instruments are fitted with an electrospray ionization (ESI) source.

For the Synapt G2 HDMS settings, the capillary voltage was set to 3 kV, the sampling cone voltage was set to 40 V, and the extraction cone was set to 4 V. The source and desolvation temperatures were 100 °C and 200 °C, respectively. No cone gas flow was used and the desolvation gas flow was set to 500 L/h. The voltages for the trap and the transfer collision energies (CE) were set to 4 V and 2 V, respectively. For “native” IM-MS spectra, the trap bias was set to 45 V. This voltage value was changed for CIU and CID experiments. For PEtP and PEO, the IM wave height was 40 V and the wave speed was set to 1200 m/s. The trap Ar gas flow was set to 2 mL/min, the He gas flow was 180 mL/min, and the N₂ pressure in the IM cell was set to 2.6 mbar. For *Pn*-PrOx, the IM wave speed was set to 1000 m/s, keeping the other settings identical. The calibration curves [38, 39] are represented in Figures S112–S114, using biomolecules as calibration substances [40–45].

The arrival time distributions were fitted with Gaussian functions in order to extract drift time values with higher reproducibility (apex of the Gaussian fit). Data treatment was performed using MassLynx v.4.1, Peakfit v.4.11, Excel 2011, and Igor Pro 6.37.

Collision Induced Unfolding (CIU) and Dissociation (CID) Using a Synapt G2 HDMS

To perform CIU and CID experiments, the trap bias voltage values of the Synapt G2 HDMS were used. Breakdown curves of the precursor ions as well as relative intensities of the product ions were sampled according to the accelerating voltage. The data represented in this work were extracted from the voltage values resulting in the highest relative intensities of the analyzed species. IM parameters were kept unchanged between non-activated “native” and CIU or CID-activated experiments.

Electron Transfer Dissociation (ETD) Using a Synapt G2 HDMS

The ETD experiments were performed in the trap cell of a Synapt G2 HDMS instrument (Waters Corp., UK), in front of the ion mobility cell. For each experiment, bicyanobenzene was used as ETD reagent and, according to the manufacturer’s protocol, its ionization settings (gas flow and discharge current) were optimized to reach an intensity of around 10^6 counts per scan. For each experiment, the trap wave velocity and trap wave height were optimized in order to maximize the ETD reaction. The IM parameters were 1200 m/s wave velocity and 40 V wave height. The IM N₂ pressure was 2.6 mbar, and the Ar trap and transfer cell gas flows were 2 mL/min.

Ion Mobility–Mass Spectrometry (IM-MS) and *is*CID Using a timsTOF

The capillary voltage of the timsTOF was set to 2500 V, the nebulizer pressure was 0.3 bar, the drying gas was set to

3.5 L/min, and the drying temperature was 200 °C. The used TIMS ramp ranged from 0.60 to 1.60 1/ K_0 with a ramp duration of 500 ms. The TIMS was calibrated online using Agilent Tune Mix [46]. The isCID voltage was set to 100 V. Both the PEO 750 g/mol and the 2000 g/mol samples were measured at 100 V isCID in order to be able to correlate both measurements. Indeed, the isCID induces a slight shift in the elution voltages or 1/ K_0 values due to the isCID voltage coupling with the TIMS funnels. On the timsTOF used for this study, it is therefore not recommended to use high isCID voltages for long experiment durations due to possible electronics overload. Only the 1+ ions that were not present in the 2000 g/mol sample at isCID = 0 V were compared to the “native” 1+ ions from the 750 g/mol sample (see text). The 1+ ions from the 750 g/mol sample were monitored over several isCID voltage values to ensure that their signals did not increase in intensity, meaning that no additional 1+ product ions were formed at isCID = 100 V, thus analyzing only the surviving 1+ ions from PEO 750 g/mol.

Data treatment was performed using DataAnalysis 5.0, VBA scripts, Peakfit v.4.11, Excel 2011, and Igor Pro 6.37.

Results and Discussions

General CID and ETD Reactivity Assessment

The first step in this study is to collisionally activate the polymer precursor ions at different accelerating voltage values. The different degradation channels can thus be assessed and the most appropriate accelerating voltage can be retained for each of the studied cases: collisionally activated (intact) precursor ions (collision induced unfolding, CIU), cation ejection species, and fragment ions (collision induced dissociation, CID). In this work, we denote as “cation ejection species” (CES) intact precursor ions having ejected/lost one or several cations without fragmenting (charge reduction). Figure 1 illustrates the studied ion activation products and the related used activation techniques. The relative intensities of such CID-formed product ions for PETP polymers at various charge states are plotted as a function of the accelerating voltage in Figure 2.

Based on the curves presented in Figure 2, the voltage ranges for performing the CID measurements are found and the appropriate voltages are used in the rest of this article.

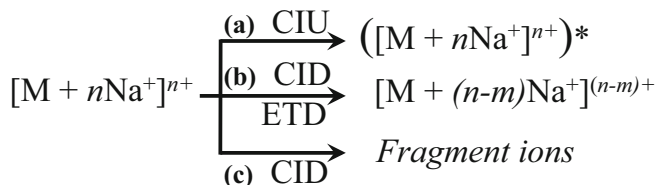


Figure 1. Illustration of the different product ions after ion activation. (a) Collision induced unfolding experiment (CIU) of the precursor ion (collisional activation). (b) Cation ejection species (CES) obtained after collision induced dissociation (CID) or electron transfer dissociation (ETD, formally ETnoD). (c) CID-obtained fragment ions

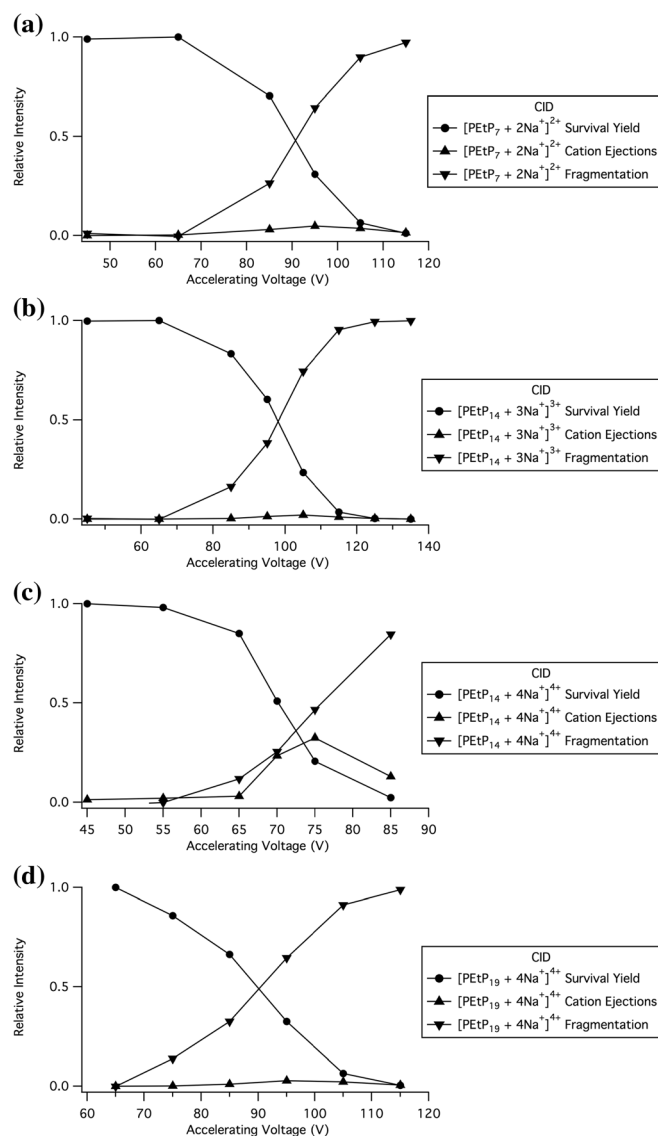


Figure 2. Evolutions of relative intensities of three precursor ions subjected to accelerating voltages in CID experiments. Different degradation pathways are observed and monitored: cation ejection species (CES) and the formation of fragment ions. (a) [PETP₇ + 2Na⁺]²⁺ precursor ion; (b) [PETP₁₄ + 3Na⁺]³⁺ precursor ion; (c) [PETP₁₄ + 4Na⁺]⁴⁺ precursor ion; (d) [PETP₁₉ + 4Na⁺]⁴⁺ precursor ion

Contrary to CID, the activation energy cannot be easily fine-tuned for the electron transfer dissociation (ETD) reaction. No preliminary assessment of the conferred activation energy is thus necessary for ETD activations.

Collisionally Activated Precursor Ions: CIU Experiments

Figure 3 compares the drift times of the collisionally activated precursor ions (CIU) to the non-activated native precursor ions. Globally, the drift time evolutions of the sampled charge states (2+ to 4+) match well, whether the ions were collisionally heated or not. Figure 3b represents the drift time (t_d) difference

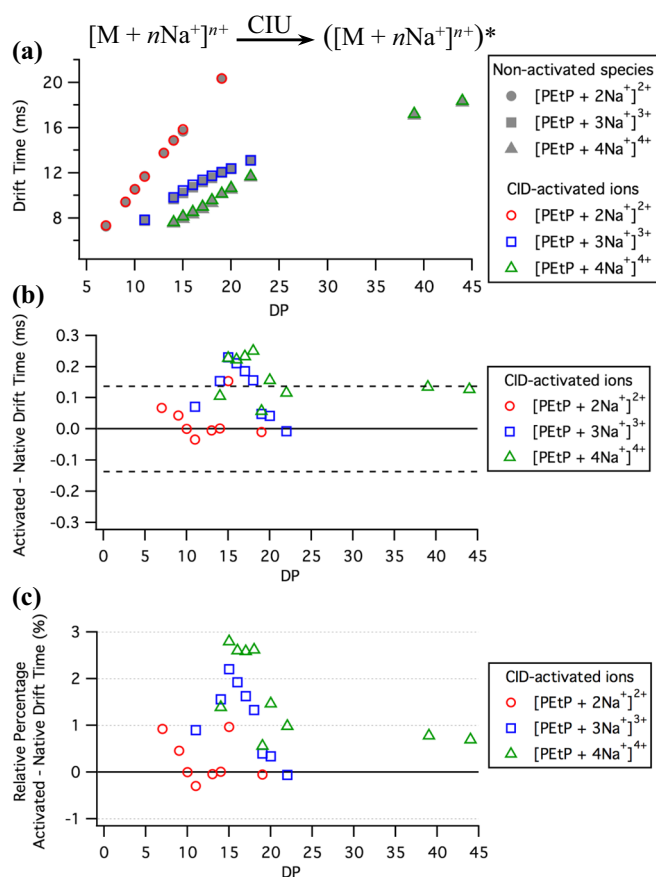


Figure 3. Comparison of collisional activation of PEtP precursor ions (CIU) and native non-activated precursor ions as a function of the DP. **(a)** Drift times plotted as a function of the DP for three charge states of PEtP. Gray markers represent native non-activated precursor ions and colored markers represent collisionally activated precursor ions. **(b)** Drift time difference between activated and non-activated polymer complexes. The dotted lines represent the instrument's acquisition bin width. **(c)** Percentage drift time deviations of activated and non-activated polymer complexes (Eq. (1))

between the activated ion and the non-activated native ion. The 1+ ion drift time differences are all found to be beyond the limit of the instrument IM resolving power, i.e., the instrument's acquisition bin width (0.1375 ms for these IM conditions). The t_d differences of several activated 2+ and 3+ ions, however, are greater than the nominal bin width. Given that the arrival time distributions are fitted with Gaussian functions in order to define the t_d values (apex of the Gaussian fit), small deviations from the bin width limit should nevertheless not be considered as significant. Interestingly, it seems that the t_d difference first increases and then decreases when the DP (degree of polymerization) increases within the 2+ and 3+ charge states. This is also demonstrated in Figure 3c where the percentage deviations of the activated ions compared to the non-activated native ions are plotted (Eq. (1)).

$$\% \text{deviation} = \frac{t_d(M^*) - t_d(M)}{t_d(M)} \times 100 \quad (1)$$

where t_d is the drift time, $t_d(M^*)$ is the drift time of the activated species (CIU collisionally activated, cation ejection species or fragment ion), and $t_d(M)$ is the drift time of the precursor (or the native intact polymer) ion.

A possible explanation for these small t_d differences after CIU could be found in Figure 2 where the higher-charged complexes (at equivalent DP value, see Figure 2b and c for DP 14) are observed to eject more intensely cations (based on the relative intensities). This trend decreases with increasing DP values because the cations become less accessible and the Coulomb repulsion between the cations decreases. Fragmentation pathways then become more significant than cation ejections (see Figure 2c and d). The opening of the complexes leading to favorable cation ejections could thus potentially explain the observed t_d deviations which increase with the charge state and then decrease within each charge state as a function of the DP. For low-DP complexes, the cations can be easily ejected without further apparent polymer chain rearrangement: no significant t_d deviation is observed (see Figure 3b and c). When the DP increases, the polymer chain has to slightly rearrange for the cation ejections to occur after CIU, leading to increasing t_d deviations (Figure 3b, c). Finally, at high DP values, the polymer is too large for cation ejections because fragmentation pathways become more favorable (Figure 2). The polymer chain does not rearrange anymore to potentially allow subsequent cation ejection, hence leading to a decrease in the t_d deviations.

All in all, the collisionally activated precursor ions do not show large t_d (or CCS, see Figure S11) deviations from the native non-activated precursor ions. This opening can also be compared to CIU experiments often performed on biomolecules [47, 48]. The CIU t_d differences observed on biomolecules seem largely superior ($\sim 10\%$ deviations or more) to the ones generally observed on PEtP ($< 3\%$ in t_d or $< 2\%$ in CCS). Specifically, the 1+ charge state and the low- or high-DP complexes for multiply charged ions seem to present robust IM behaviors. This is of crucial interest for the robustness and reproducibility of IM calibration strategies based on synthetic homopolymers [38, 49], especially if based solely on singly charged synthetic homopolymers [38]. Our data indeed suggest that the activation energy provided to the polymer ions by collisions with, e.g., the drying gas does not affect their resulting apparent CCS values. The measured drift times for these polymer ions then become independent of the ion optics of the instruments, as we already presented in a previous study [29]. It should, however, be noted that we do not conclude on the precise three-dimensional arrangement of the polymer chain in the complex, but rather on the measured IM-MS drift times and the average CCS values.

CID and ETnoD: Cation Ejection Species (CES)

In order to push the polymer ion shape comparisons with native non-activated polymer ions further, cation ejection species were investigated. The CES represent charge-reduced polymer ions without polymer fragmentation (see Figure 1b). They can

be yielded using both CID and ETD (formally ETnoD). Figure S13 describes the yields of the cation ejections according to the precursor charge state and the DP. As briefly discussed above, the cation ejections increase with the increasing charge state (more ejection possibilities) and decrease with the increasing DP (fragmentation pathways become more favorable). Using CID, both one and two cations are ejected from the sampled polymer ions (from 4+ to 3+ and 2+, from 3+ to 2+ and 1+, from 2+ to 1+). When the DP increases, the signal intensity of the CES from two cation ejections decreases before the signal of the CES from one cation ejection disappears. Using ETD (i.e., ETnoD), only single charge ejections are observed on the sampled polymer ions (from 4+ to 3+ and from 3+ to 2+; see Figure S14). The 2+ ions do not exhibit any ETD reaction (data not shown).

Figure 4 exhibits the t_d evolutions and t_d differences of the CES formed using CID and ETD, compared to the native non-activated ions. The arrival time distributions of the formed 1+ species (see Figure S13) cannot be interpreted because they travel too slowly through the IM cell and the species from the previous IM cycle are eluted during the following next IM injection cycle (rollover in the traveling wave Synapt G2 HDMS instrument). Figure 4 shows that the overall t_d evolutions of the CES overlap with their respective native non-activated counterparts. More

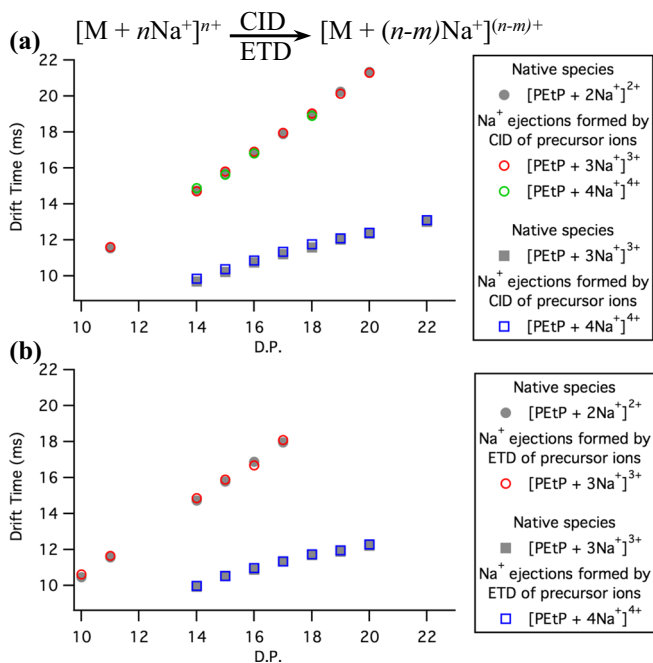


Figure 4. Comparison of PETp cation ejection species and native non-activated polymer ions as a function of the DP. (a) Represents CID-obtained CES and (b) represents ETnoD-obtained CES. (a) Drift times of 2+ ions (native non-activated ions and CID CES from both 3+ and 4+ precursor ions) and of 3+ species (native non-activated ions and CID CES from 4+ precursor ions). (b) Drift times of 2+ species (native ions and ETnoD CES from 3+ precursor ions) and of 3+ species (native ions and ETnoD CES from 4+ precursor ions). Gray markers represent native non-activated precursor ions and colored markers represent CID or ETnoD-formed CES

precisely, all measured t_d differences are smaller than (or very close to) the limiting acquisition bin width. In terms of percentage deviations (Eq. (1)) from the native non-activated ions, the CID- and ETD-formed CES are mostly beyond the 1% deviation (Figure S15). Even though the energy repartition during CID activation leads to the internal energy being distributed over all normal modes of vibration (ergodic) and ETD is based on localized ion–ion reactions (non-ergodic), no distinction between the native non-activated ions and the CES can be made based on CCS or drift time values. The CES formed by CID and ETD are thus also indistinguishable.

CID Fragment Ions

Thus far, polymer ions showed to have robust CCS values and/or to yield shapes with similar CCS values than their native counterparts, whether being collisionally activated (CIU) or having ejected cations (CES from CID or ETnoD). Given that no significant differences between the shapes of the product ions formed by either CID or ETD were found, we continue to explore only the CID activation in this section. Here, we provided the maximum internal energy to the ions, i.e., until reaching the fragmentation threshold (Figures 1c and 2). The formed species should thus have enough internal energy to sample their conformational space [50] until being trapped in their conformations (owing to thermalization in the IM cell [51]). The fragment ions which we chose to analyze had identical m/z and charge state values than intact polymer ions. They were compared to their native intact counterparts in terms of drift time or CCS, without making any assumption on the fragment ion identity: depolymerization-type fragments or any fragments with differing chemical structures but identical m/z ratios and charge states could thus be mixed in the measured arrival time distributions.

Figure 5a represents the t_d differences of CID-formed product ions from [PETp₂₂ + 4Na⁺]⁴⁺ (i.e., fragments) compared to native non-activated (intact) polymer ions with identical m/z and charge states. It exhibits that most of the analyzed fragment ions cannot be differentiated within the limiting acquisition bin width. Figures S16 and S17, as well as Table S11 show the t_d and CCS evolutions, as well as the differences and the percentage deviations of the fragment ions. In terms of percentage deviations, only three ions exceed a 2% t_d deviation (t_d deviation < 3%; CCS deviation < 1.6%) compared to the native intact ions, with many species being below the 1% t_d or CCS deviation (Figure S16.c. and Table S11).

In order to verify whether other polymers also yield indistinguishable t_d values of their fragment ions compared to native intact polymer ions of the same m/z and charge state, Pn-PrOx and PEO were also investigated. Figure 5b and c represent the t_d differences of fragment ions from [Pn-PrOx₂₉ + 3Na⁺]³⁺ and [PEO₄₆ + 4Na⁺]⁴⁺ compared to the respective native intact ions with the same m/z and charge state values. Figures S18 to S111, as well as Tables S12 and S13 show the t_d and CCS evolutions with the differences and percentage deviations of the analyzed species.

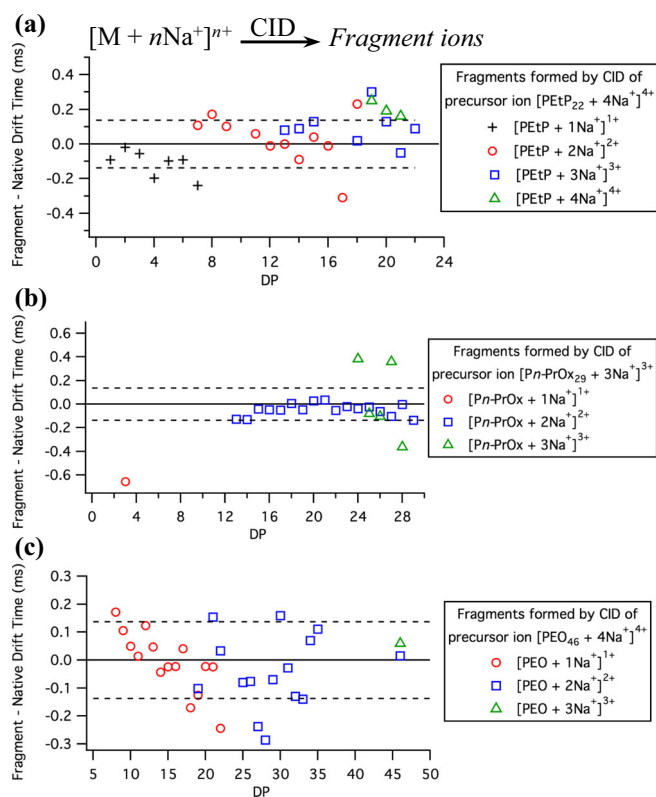


Figure 5. Comparison of drift time differences between CID-obtained fragment ions and native intact polymer ions as a function of the DP. The analyzed fragment ions yield m/z and charge state values identical to smaller native intact polymer ions. The dotted lines represent the instrument's acquisition bin width. Fragment ions formed from the precursor ions: (a) $[\text{PEtP}_{22} + 4\text{Na}^+]^{4+}$; (b) $[\text{Pn-PrOx}_{29} + 3\text{Na}^+]^{3+}$; (c) $[\text{PEO}_{46} + 4\text{Na}^+]^{4+}$

Most of the formed product ions from $[\text{Pn-PrOx}_{29} + 3\text{Na}^+]^{3+}$ are doubly charged. All the 2+ product ions have t_d values which are indistinguishable within the bin width limit from an equivalent non-activated native (intact) polymer ion of the same m/z and charge state. Out of the five formed 3+ fragment ions, two are within the bin width limit. Three fragments show an increased difference between the product ion t_d and the native ion t_d . Their percentage t_d deviations are around 3% (or $\sim 2\%$ CCS deviations). These differences could be due to stronger hydrogen bonding interactions present in Pn-PrOx than in PEtP. Indeed, the poly(2-*n*-propyl-2-oxazoline) side chains are constituted by amide functions which could form different stable conformations in the gas phase [30, 33, 52–56]. Interestingly however, not all the formed 3+ fragment ions exhibit such t_d deviations. Concerning the 1+ product ions, only two fragment ions with m/z ratios potentially matching the m/z ratios of 1+ intact native polymer ions were formed (Figure S18.a. and S19.a.). Only one of those intact native ions is detected during the non-activated IM-MS experiment, the other one not being formed during ESI. A $\sim 9\%$ t_d deviation (or $\sim 6\%$ CCS deviation) is to be noted for the product ion whose native counterpart exists (Table S12). Based on these

observations, the formed 1+ product ions could in fact be clusters of different polymer chain fragments instead of a bound polymer chain. Such clusters could be stable due to the hydrogen bonding interactions favored by the amide functions.

The analyzed product ions formed by CID from $[\text{PEO}_{46} + 4\text{Na}^+]^{4+}$ are both singly and doubly charged, with one triply charged fragment being formed. The vast majority of the t_d differences between the formed product ions and their intact native counterparts are within the bin width limit. Most product ions show t_d deviations smaller than 1% (Figures S110.c, S111.c. and Table S13). Only three ions exhibit a t_d deviation larger than 2% (but still $< 3\%$) while the CCS percentage deviations are all smaller than 1.5%. It can be noted that especially the t_d values of these 1+ PEO product ions are in good agreement with the intact native polymer ions.

CID Fragment Ions with High Resolving Power IM-MS

Given that the Synapt G2 HDMS ion mobility–mass spectrometer has a limited resolving power ($\text{CCS}/\Delta\text{CCS}$) of around 40–50 [57], measurements with a higher IM resolving power instrument were performed (TIMS) [58, 59]. The advantage of the Synapt G2 HDMS setup is the possibility of isolating the ions using a quadrupole m/z filter before CID or ETD activation and IM separation. The TIMS instrument (timsTOF; Bruker), however, does not allow for m/z isolation prior to collisional activation. Therefore, only in-source CID (isCID) can be performed on the whole polymer sample at once. However, the voltage gradient during the isCID experiment using the timsTOF operating in IM-MS mode is applied from the ion source to the TIMS funnels and could lead to artifacts concerning the elution voltage measurements. We used two different PEO samples, one at 750 g/mol and a second at 2000 g/mol: the first sample contains small polymer chains leading to 1+ charge states, which the 2000 g/mol sample does not contain. By performing isCID on the 2000 g/mol sample, we can thus form the fragments with identical m/z and charge state values than the 1+ pseudomolecular ions which are natively present in the 750 g/mol sample (see also “Materials and Methods” section). We were hence able to compare intact native polymer ions with CID-formed product ions on a high IM resolving power instrument. Here, we do not control the identity of the precursor ions leading to the fragment ions. This should enable us to evaluate whether the small differences observed on the low IM resolving power instrument could still be due to small shape variations.

Figure 6 represents the reduced mobility (K_0) of native (750 g/mol sample) and isCID-formed (2000 g/mol sample) 1+ ions, as well as their K_0 differences and percentage deviations. Only small K_0 deviations are observed using the TIMS instrument. They do not surpass 1% (Figure 6c). If these deviations are not due to artifacts of the isCID experiment, then they necessitate a resolving power of at least 170 (or even higher) for them to be noticed. The shapes of the isCID-formed

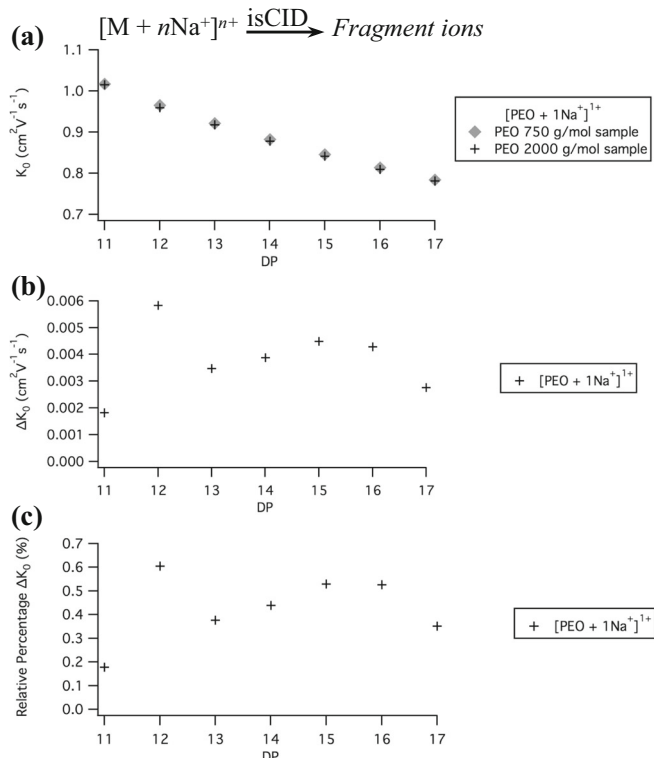


Figure 6. Comparison of isCID-obtained fragment ions from PEO 2000 g/mol sample precursor ions with intact native polymer ions from a PEO 750 g/mol sample as a function of the DP. (a) K_0 plotted as a function of the DP. Gray markers represent intact native polymer ions and colored markers represent fragment ions. (b) K_0 difference between fragment ions and intact native polymer ions. (c) Percentage K_0 deviations of fragment ions and intact native polymer ions (Eq. (1) with K_0 instead of t_d)

1+ product ions thus do not seem to significantly deviate from the intact native [PEO + 1Na⁺]¹⁺ counterparts when measured using IM. This confirms that the t_d differences are indeed unresolved on the Synapt G2 HDMS instrument.

Implications for IM Calibrations

IM calibrations based on biomolecules have long suffered from reproducibility issues. The measured drift times often depend on the ion activation and therefore on the instrument/experimental settings [47, 48, 52, 55, 60–64]. This is also exhibited in CIU studies [47, 48]. Apart from yielding spherically shaped ions with minimized sequence influences on the CCS, polymer IM calibration strategies based on 1+ ions [38] are thus able to correct the biases of large drift time variations according to the instrument settings and the subsequent ion activation [29]. Indeed, the majority of the studied product ions did not exhibit large drift time (or CCS or K_0) differences compared to their native counterparts with identical m/z and charge state.

This then leads to new applications of the IM calibrating ions. For instance, CIU experiments (on, e.g., biomolecules) can be accurately calibrated for CCS or K_0 value extraction using (1+) polymer calibrants [38]. Furthermore, the 1+

polymer ion calibrating substances can be used whatever the experimental settings [29, 38]. If for example harsh ionization source conditions have to be employed, a high-DP sample could be used to create “in situ” the low-DP 1+ calibrating ions, as shown in the TIMS experiments.

Implications for Gas-Phase Structures

The precursor ions used in this study sampled different DP values and charge states. These precursor ions thus sampled different ranges of the CCS evolutions as a function of the DP: ions from the common trend line [30, 34] as well as ions with CCS values before, during, and after the structural rearrangements of the polymer ions [27–29, 34, 65, 66]. All precursor ions, regardless of their initial CCS, were able to yield CES (CID and ETnoD) or fragment ions having CCS values very close to the native polymer ions of the same m/z and charge state, regardless of the formed ion’s CCS being part of the common trend line, the structural rearrangements, or CCS evolutions. The CCS values were hence essentially driven by the charge state/Coulomb repulsion.

This could give insights into the possible three-dimensional structures of the precursor and CES/fragment ions. On the one hand, the ion shape formation could be rapid and all shapes could be quickly reformed after activation, cation ejection, or fragmentation. On the other hand, the different ion shapes could all be related, meaning that chain fragmentation occurs at preferential sites, which directly yields the “new” native ion shape, without any structure changes in the gas phase.

Implications for IM-MS of Polymers

Fragment ions yielding drift times (or CCS or K_0 values) close to the values of native intact polymer ions allow the analysis of high-DP samples using the polymer CCS prediction method [34]. The CCS prediction method is based on establishing polymer CCS trends in order to interpret the polymer topology, monomer branching, etc. In this method, it is useful to analyze the CCS evolutions of low-DP polymer ions to confidently establish the common trend line and further CCS trends. This can hence be performed even for high-DP samples by, e.g., prior polymer digestion, degradation, or “in situ” MSⁿ fragmentation. A high-DP polymer sample, e.g., PEO 5000 g/mol, can thus yield the CCS evolutions of a low-DP sample, e.g., PEO 750 g/mol, thus allowing accessing all CCS trends with only one high-DP sample. Reference CCS trends of linear polymers could then be easily established.

Prospects for Improving CCS Calculations

Finally, polymer ions could be used as model systems to probe ion–drift gas interaction potentials. In literature, CCS values of 1+ polymer ions (PEO) have been measured as a function of the temperature using a physically heated homemade drift tube instrument [67, 68]. Such experiments could be reproduced on more recent variable temperature IM-MS instruments [69, 70] with higher IM resolving power. CID, ETD, or even other

activation experiments coupled to IM, as performed in this work, should then also be performed on such new IM-MS instruments. The potential CCS differences in variable temperature IM-MS experiments could then be traced back to either actual shape variations or to the temperature influence on the ion–drift gas particle interaction potential. This could then help improve CCS calculation algorithms [71–73] by possibly improving or refining the descriptions of interaction potentials or of the momentum scattering coefficient between the drift gas particle and the ion.

Conclusions

In this work, we activated synthetic homopolymer ions using different gas-phase techniques and we evaluated their resulting ion mobility drift times (or CCS). First, we activated polymer ions using the so-called collision induced unfolding CIU experiments and compared the drift times of intact polymer ions with and without collisional activation. Second, CID and ETD (formally ETnD) were used to induce precursor ion fragmentation. Here, we analyzed two types of product ions. On the one hand, we analyzed the product ions that have ejected/lost one or multiple cations while retaining an intact polymer chain (CES). On the other hand, we analyzed the product ions which yield m/z and charge state values identical to “native” non-activated intact polymer ions. The drift times (or CCS) of the CES and the product ions were then compared to the drift times (or CCS) of the native non-activated intact polymer ions with identical m/z and charge state. All experiments were performed on PETP, with additional IM fragment analysis for two other synthetic homopolymers: *Pn*-PrOx and PEO.

Concerning the CIU-activated precursor ions, we observed either no significant or only small drift time variations upon collisional activation. Most drift times were beyond the instrumental IM resolving power. Some ions exhibited small drift time (or CCS) variations according to the charge state and DP range, with the variations not surpassing 2% in CCS.

Regarding the CES product ions, no drift time distinction could be made between CES ions and native intact polymer ions. This result was independent of the activation method being ergodic (CID) or non-ergodic (ETD).

Fragment product ions (CID) were also shown to be mostly indistinguishable from native intact non-activated polymer ion IM with identical m/z and charge states. Out of all the analyzed ions, only one differed by 9% in CCS, while the other analyzed ions differed by less than 2–3% in CCS. In order to check if these observations still hold on a higher resolving power IM-MS instrument, singly charged PEO was then re-evaluated on a TIMS instrument instead of the Synapt G2 HDMS instrument used for the rest of this study. Here, no significant K_0 changes were observed from native intact ions compared to CID-formed product ions with identical m/z and charge state. If the observed small deviations are indeed significant and not artifacts from the *is*CID experiments, then the deviations are only apparent at resolving powers higher than 170.

These results led to several conclusions and discussions. For polymer IM-MS analyses, it is interesting to note that whatever the precursor ion CCS (i.e., before, after, or during the structural rearrangement), they can yield product ions with CCS values before, after, or during the structural rearrangement. Polymer CCS trend predictions at low DPs [34] can then be accessed using high-DP samples. Furthermore, conclusions on the polymer ion folding can be drawn. The folding is either quicker than the IM analysis (migration) time or it is related through all DP and charge states. The latter translates, e.g., into preferential fragmentation sites which, when cleaved, would directly lead to the expected shapes according to the polymer DP and charge state.

Furthermore, the results demonstrated the robustness and reproducibility of the polymer ion drift times and CCS (or K_0) values. This makes them well suited as IM calibrating substances, especially the singly charged (PEO) polymer ions [38, 49]. These ions could even be created in the gas phase as fragmentation product ions from higher DP and higher charge state precursor ions, thus also opening the way for accurate IM calibrations in CIU experiments.

Lastly, if the polymer CCS values are independent of the internal ion energy, then CCS changes measured during variable temperature IM-MS experiments should only be due to changes in the ion–drift gas particle interaction potentials or in the scattering coefficient. Polymer ions could then be used for improving these theoretical chemistry interaction descriptors.

Acknowledgements

The authors thank the F.R.S.-FNRS for the financial support (F.R.I.A.). R.H. acknowledges financial support from FWO and Ghent University.

Publisher's Note Springer Nature remains neutral with regard to jurisdictional claims in published maps and institutional affiliations.

References

1. Floris, F., Vallotto, C., Chiron, L., Lynch, A.M., Barrow, M.P., Delsuc, M.A., O'Connor, P.B.: Polymer analysis in the second dimension: preliminary studies for the characterization of polymers with 2D MS. *Anal. Chem.* **89**, 9892–9899 (2017)
2. Wesdemiotis, C., Solak, N., Polce, M.J., Dabney, D.E., Chaicharoen, K., Katzenmeyer, B.C.: Fragmentation pathways of polymer ions. *Mass Spectrom. Rev.* **30**, 523–529 (2011)
3. Baumgaertel, A., Altuntaş, E., Kempe, K., Crecelius, A., Schubert, U.S.: Characterization of different poly(2-oxazoline) block copolymers by MALDI-TOF MS/MS and ESI-Q-TOF MS/MS. *J. Polym. Sci. A Polym. Chem.* **48**, 5533–5540 (2010)
4. Crotty, S., Gerişlioğlu, S., Endres, K.J., Wesdemiotis, C., Schubert, U.S.: Polymer architectures via mass spectrometry and hyphenated techniques: a review. *Anal. Chim. Acta.* **932**, 1–21 (2016)
5. Yol, A.M., Dabney, D.E., Wang, S.F., Laurent, B.A., Foster, M.D., Quirk, R.P., Grayson, S.M., Wesdemiotis, C.: Differentiation of linear and cyclic polymer architectures by MALDI tandem mass spectrometry (MALDI-MS2). *J. Am. Soc. Mass Spectrom.* **24**, 74–82 (2013)

6. Knop, K., Jahn, B.O., Hager, M.D., Crecelius, A., Gottschaldt, M., Schubert, U.S.: Systematic MALDI-TOF CID investigation on different substituted mPEG 2000. *Macromol. Chem. Phys.* **211**, 677–684 (2010)
7. Girod, M., Phan, T.N.T., Charles, L.: Microstructural study of a nitroxide-mediated poly(ethylene oxide)/polystyrene block copolymer (PEO-b-PS) by electrospray tandem mass spectrometry. *J. Am. Soc. Mass Spectrom.* **19**, 1163–1175 (2008)
8. Jeanne Dit Fouque, D., Maroto, A., Memboeuf, A.: Purification and quantification of an isomeric compound in a mixture by collisional excitation in multistage mass spectrometry experiments. *Anal. Chem.* **88**, 10821–10825 (2016)
9. Memboeuf, A., Nasioudis, A., Indelicato, S., Pollreis, F., Kuki, Á., Kéki, S., Van Den Brink, O.F., Vékey, K., Drahos, L.: Size effect on fragmentation in tandem mass spectrometry. *Anal. Chem.* **82**, 2294–2302 (2010)
10. Josse, T., De Winter, J., Dubois, P., Coulembier, O., Gerbaux, P., Memboeuf, A.: A tandem mass spectrometry-based method to assess the architectural purity of synthetic polymers: a case of a cyclic polylactide obtained by click chemistry. *Polym. Chem.* **6**, 64–69 (2015)
11. Memboeuf, A., Jullien, L., Lartia, R., Brasme, B., Gimbert, Y.: Tandem mass spectrometric analysis of a mixture of isobars using the survival yield technique. *J. Am. Soc. Mass Spectrom.* **22**, 1744–1752 (2011)
12. Nasioudis, A., Memboeuf, A., Heeren, R.M.A., Smith, D.F., Vékey, K., Drahos, L., Van Den Brink, O.F.: Discrimination of polymers by using their characteristic collision energy in tandem mass spectrometry. *Anal. Chem.* **82**, 9350–9356 (2010)
13. Katzenmeyer, B.C., Cool, L.R., Williams, J.P., Craven, K., Brown, J.M., Westdemiotis, C.: Electron transfer dissociation of sodium cationized polyesters: reaction time effects and combination with collisional activation and ion mobility separation. *Int. J. Mass Spectrom.* **378**, 303–311 (2015)
14. Burel, A., Carapito, C., Lutz, J.-F., Charles, L.: MS-DECODER: milliseconds sequencing of coded polymers. *Macromolecules.* **50**, 8290–8296 (2017)
15. Charles, L., Laure, C., Lutz, J.-F., Roy, R.K.: MS/MS sequencing of digitally encoded poly(alkoxyamine amide)s. *Macromolecules.* **48**, 4319–4328 (2015)
16. Chendo, C., Phan, T.N.T., Rollet, M., Gignes, D., Charles, L.: Addition of ammonium to polylactides to modify their dissociation behavior in collision-induced dissociation. *Rapid Commun. Mass Spectrom.* **32**, 423–430 (2018)
17. Amalian, J.-A., Trinh, T.T., Lutz, J.-F., Charles, L.: MS/MS digital readout: analysis of binary information encoded in the monomer sequences of poly(triazole amide)s. *Anal. Chem.* **88**, 3715–3722 (2016)
18. Amalian, J.-A., Poyer, S., Petit, B.E., Telitel, S., Monnier, V., Karamessini, D., Gignes, D., Lutz, J.-F., Charles, L.: Negative mode MS/MS to read digital information encoded in sequence-defined oligo(urethane)s: a mechanistic study. *Int. J. Mass Spectrom.* **421**, 271–278 (2017)
19. Kaczorowska, M.A., Cooper, H.J.: Electron capture dissociation, electron detachment dissociation, and collision-induced dissociation of polyamidoamine (PAMAM) dendrimer ions with amino, amidoethanol, and sodium carboxylate surface groups. *J. Am. Soc. Mass Spectrom.* **19**, 1312–1319 (2008)
20. Kaczorowska, M.A., Cooper, H.J.: Characterization of polyphosphoesters by Fourier transform ion cyclotron resonance mass spectrometry. *J. Am. Soc. Mass Spectrom.* **20**, 2238–2247 (2009)
21. Cerda, B., Horn, D., Breuker, K., Carpenter, B., McLafferty, F.: Electron capture dissociation of multiply-charged oxygenated cations. A nonergodic process. *Eur. J. Mass Spectrom.* **5**, 335 (1999)
22. Cerda, B.A., Breuker, K., Horn, D.M., McLafferty, F.W.: Charge/radical site initiation versus coulombic repulsion for cleavage of multiply charged ions. Charge solvation in poly(alkene glycol) ions. *J. Am. Soc. Mass Spectrom.* **12**, 565–570 (2001)
23. Cerda, B.A., Horn, D.M., Breuker, K., McLafferty, F.W.: Sequencing of specific copolymer oligomers by electron-capture-dissociation mass spectrometry. *J. Am. Chem. Soc.* **124**, 9287–9291 (2002)
24. Altuntaş, E., Knop, K., Tauhardt, L., Kempe, K., Crecelius, A.C., Jäger, M., Hager, M.D., Schubert, U.S.: Tandem mass spectrometry of poly(ethylene imine)s by electrospray ionization (ESI) and matrix-assisted laser desorption/ionization (MALDI). *J. Mass Spectrom.* **47**, 105–114 (2012)
25. Altuntaş, E., Weber, C., Schubert, U.S.: Detailed characterization of poly(2-ethyl-2-oxazoline)s by energy variable collision-induced dissociation study. *Rapid Commun. Mass Spectrom.* **27**, 1095–1100 (2013)
26. Trimpin, S., Clemmer, D.E.: Ion mobility spectrometry/mass spectrometry snapshots for assessing the molecular compositions of complex polymeric systems. *Anal. Chem.* **80**, 9073–9083 (2008)
27. Trimpin, S., Plasencia, M., Isailovic, D., Clemmer, D.E.: Resolving oligomers from fully grown polymers with IMS-MS. *Anal. Chem.* **79**, 7965–7974 (2007)
28. Larriba, C., Fernandez De La Mora, J.: The gas phase structure of coulombically stretched polyethylene glycol ions. *J. Phys. Chem. B.* **116**, 593–598 (2012)
29. Haler, J.R.N., Massonnet, P., Chirot, F., Kune, C., Comby-Zerbino, C., Jordens, J., Honing, M., Mengerink, Y., Far, J., Dugourd, P., De Pauw, E.: Comparison of different ion mobility setups using poly(ethylene oxide) PEO polymers: drift tube, TIMS, and T-wave. *J. Am. Soc. Mass Spectrom.* **29**, 114–120 (2018)
30. Haler, J.R.N., Far, J., Aqil, A., Claegeboudt, J., Tomczyk, N., Giles, K., Jérôme, C., De Pauw, E.: Multiple gas-phase conformations of a synthetic linear poly(acrylamide) polymer observed using ion mobility–mass spectrometry. *J. Am. Soc. Mass Spectrom.* **28**, 2492–2499 (2017)
31. Hoskins, J.N., Trimpin, S., Grayson, S.M.: Architectural differentiation of linear and cyclic polymeric isomers by ion mobility spectrometry–mass spectrometry. *Macromolecules.* **44**, 6915–6918 (2011)
32. Morsa, D., Defize, T., Dehareng, D., Jérôme, C., De Pauw, E.: Polymer topology revealed by ion mobility coupled with mass spectrometry. *Anal. Chem.* **86**, 9693–9700 (2014)
33. Duez, Q., Josse, T., Lemaux, V., Chirot, F., Choi, C.M., Dubois, P., Dugourd, P., Cornil, J., Gerbaux, P., De Winter, J.: Correlation between the shape of the ion mobility signals and the stepwise folding process of polylactide ions. *J. Mass Spectrom.* **52**, 133–138 (2017)
34. Haler, J.R.N., Morsa, D., Lecomte, P., Jérôme, C., Far, J., De Pauw, E.: Predicting ion mobility–mass spectrometry trends of polymers using the concept of apparent densities. *Methods.* **144**, 125–133 (2018)
35. Westdemiotis, C.: Multidimensional mass spectrometry of synthetic polymers and advanced materials. *Angew. Chem. Int. Ed.* **56**, 1452–1464 (2017)
36. Larriba, C., De La Mora, J.F., Clemmer, D.E.: Electrospray ionization mechanisms for large polyethylene glycol chains studied through tandem ion mobility spectrometry. *J. Am. Soc. Mass Spectrom.* **25**, 1332–1345 (2014)
37. de la Rosa, V.R., Tempelaar, S., Dubois, P., Hoogenboom, R., Mespouille, L.: Poly(2-ethyl-2-oxazoline)-block-polycarbonate block copolymers: from improved end-group control in poly(2-oxazoline)s to chain extension with aliphatic polycarbonate through a fully metal-free ring-opening polymerisation process. *Polym. Chem.* **7**, 1559–1568 (2016)
38. Haler, J.R.N., Kune, C., Massonnet, P., Comby-Zerbino, C., Jordens, J., Honing, M., Mengerink, Y., Far, J., De Pauw, E.: Comprehensive ion mobility calibration: poly(ethylene oxide) polymer calibrants and general strategies. *Anal. Chem.* **89**, 12076–12086 (2017)
39. Ruotolo, B.T., Benesch, J.L.P., Sandercock, A.M., Hyung, S.-J., Robinson, C.V.: Ion mobility–mass spectrometry analysis of large protein complexes. *Nat. Protoc.* **3**, 1139–1152 (2008)
40. Counterman, A.E., Valentine, S.J., Srebalus, C.A., Henderson, S.C., Hoaglund, C.S., Clemmer, D.E.: High-order structure and dissociation of gaseous peptide aggregates that are hidden in mass spectra. *J. Am. Soc. Mass Spectrom.* **9**, 743–759 (1998)
41. Bush, M.F., Campuzano, I.D.G., Robinson, C.V.: Ion mobility mass spectrometry of peptide ions: effects of drift gas and calibration strategies. *Anal. Chem.* **84**, 7124–7130 (2012)
42. Valentine, S.J., Counterman, A.E., Clemmer, D.E.: Conformer-dependent proton-transfer reactions of ubiquitin ions. *J. Am. Soc. Mass Spectrom.* **8**, 954–961 (1997)
43. Shelimov, K.B., Jarrold, M.F.: Vacuum : an activation barrier for gas-phase protein folding. *J. Am. Chem. Soc.* **119**, 2987–2994 (1997)
44. Chen, Y.L., Collings, B.A., Douglas, D.J.: Collision cross sections of myoglobin and cytochrome c ions with Ne, Ar, and Kr. *J. Am. Soc. Mass Spectrom.* **8**, 681–687 (1997)
45. Valentine, S.J., Anderson, J.G., Ellington, A.D., Clemmer, D.E.: Disulfide-intact and -reduced lysozyme in the gas phase: conformations and pathways of folding and unfolding. *J. Phys. Chem. B.* **101**, 3891–3900 (1997)
46. Flanagan, J.M.: Mass spectrometry calibration using homogeneously substituted fluorinated triazatriphosphorines. US 5872357 A (1999)

47. Zhong, Y., Han, L., Ruotolo, B.T.: Collisional and coulombic unfolding of gas-phase proteins: high correlation to their domain structures in solution. *Angew. Chem. Int. Ed.* **53**, 9209–9212 (2014)
48. Tian, Y., Han, L., Buckner, A.C., Ruotolo, B.T.: Collision induced unfolding of intact antibodies: rapid characterization of disulfide bonding patterns, glycosylation, and structures. *Anal. Chem.* **87**, 11509–11515 (2015)
49. Duez, Q., Chirof, F., Liénard, R., Josse, T., Choi, C.M., Coulembier, O., Dugourd, P., Cornil, J., Gerbaux, P., De Winter, J.: Polymers for traveling wave ion mobility spectrometry calibration. *J. Am. Soc. Mass Spectrom.* **28**, 2483–2491 (2017)
50. Lermyte, F., Łącki, M.K., Valkenburg, D., Gambin, A., Sobott, F.: Conformational space and stability of ETD charge reduction products of ubiquitin. *J. Am. Soc. Mass Spectrom.* **28**, 69–76 (2017)
51. Morsa, D., Gabelica, V., De Pauw, E.: Fragmentation and isomerization due to field heating in traveling wave ion mobility spectrometry. *J. Am. Soc. Mass Spectrom.* **25**, 1384–1393 (2014)
52. Counterman, A.E., Clemmer, D.E.: Anhydrous polyproline helices and globules. *J. Phys. Chem. B.* **108**, 4885–4898 (2004)
53. Counterman, A.E., Clemmer, D.E.: Gas phase polyalanine: assessment of $i \rightarrow i + 3$ and $i \rightarrow i + 4$ helical turns in $[\text{Alan} + 4\text{H}]^{4+}$ ($n = 29\text{--}49$) ion. *J. Phys. Chem. B.* **106**, 12045–12051 (2002)
54. Breaux, G.A., Jarrold, M.F.: Probing helix formation in unsolvated peptides. *J. Am. Chem. Soc.* **125**, 10740–10747 (2003)
55. Counterman, A.E., Clemmer, D.E.: Compact \rightarrow extended helix transitions of polyalanine in vacuo. *J. Phys. Chem. B.* **107**, 2111–2117 (2003)
56. Rossi, M., Blum, V., Kupser, P., Von Helden, G., Bierau, F., Pagel, K., Meijer, G., Scheffler, M.: Secondary structure of Ac-Alan-LysH⁺ polyalanine peptides ($n = 5, 10, 15$) in vacuo: helical or not? *J. Phys. Chem. Lett.* **1**, 3465–3470 (2010)
57. Giles, K., Williams, J.P., Campuzano, I.: Enhancements in travelling wave ion mobility resolution. *Rapid Commun. Mass Spectrom.* **25**, 1559–1566 (2011)
58. Ridgeway, M.E., Lubeck, M., Jordens, J., Mann, M., Park, M.A.: Trapped ion mobility spectrometry: a short review. *Int. J. Mass Spectrom.* **425**, 22–35 (2018)
59. Michelmann, K., Silveira, J.A., Ridgeway, M.E., Park, M.A.: Fundamentals of trapped ion mobility spectrometry. *J. Am. Soc. Mass Spectrom.* **26**, 14–24 (2014)
60. Badman, E.R., Myung, S., Clemmer, D.E.: Evidence for unfolding and refolding of gas-phase cytochrome c ions in a Paul trap. *J. Am. Soc. Mass Spectrom.* **16**, 1493–1497 (2005)
61. Chen, S.H., Russell, D.H.: How closely related are conformations of protein ions sampled by IM-MS to native solution structures? *J. Am. Soc. Mass Spectrom.* **26**, 1433–1443 (2015)
62. Bornschein, R.E., Niu, S., Eschweiler, J., Ruotolo, B.T.: Ion mobility–mass spectrometry reveals highly-compact intermediates in the collision induced dissociation of charge-reduced protein complexes. *J. Am. Soc. Mass Spectrom.* **27**, 41–49 (2016)
63. Sun, Y., Vahidi, S., Sowole, M.A., Konermann, L.: Protein structural studies by traveling wave ion mobility spectrometry: a critical look at electrospray sources and calibration issues. *J. Am. Soc. Mass Spectrom.* **27**, 31–40 (2016)
64. Hudgins, R.R., Mao, Y., Ratner, M.a., Jarrold, M.F.: Conformations of Gly(n)H⁺ and ala(n)H⁺ peptides in the gas phase. *Biophys. J.* **76**, 1591–1597 (1999)
65. De Winter, J., Lemaire, V., Ballivian, R., Chirof, F., Coulembier, O., Antoine, R., Lemoine, J., Cornil, J., Dubois, P., Dugourd, P., Gerbaux, P.: Size dependence of the folding of multiply charged sodium cationized poly(lactides) revealed by ion mobility mass spectrometry and molecular modelling. *Chem. A Eur. J.* **17**, 9738–9745 (2011)
66. Tintaru, A., Chendo, C., Wang, Q., Viel, S., Quéléver, G., Peng, L., Posocco, P., Pricl, S., Charles, L.: Conformational sensitivity of conjugated poly(ethylene oxide)-poly(amidoamine) molecules to cations adducted upon electrospray ionization—a mass spectrometry, ion mobility and molecular modeling study. *Anal. Chim. Acta.* **808**, 163–174 (2014)
67. von Helden, G., Wytttenbach, T., Bowers, M.T.: Inclusion of a MALDI ion source in the ion chromatography technique: conformational information on polymer and biomolecular ions. *Int. J. Mass Spectrom. Ion Process.* **146–147**, 349–364 (1995)
68. Wytttenbach, T., Von Helden, G., Batka, J.J., Carlat, D., Bowers, M.T.: Effect of the long-range potential on ion mobility measurements. *J. Am. Soc. Mass Spectrom.* **8**, 275–282 (1997)
69. Ujma, J., Giles, K., Morris, M., Barran, P.E.: New high resolution ion mobility mass spectrometer capable of measurements of collision cross sections from 150 to 520 K. *Anal. Chem.* **88**, 9469–9478 (2016)
70. Dickinson, E.R., Jurneczko, E., Pacholarz, K.J., Clarke, D.J., Reeves, M., Ball, K.L., Hupp, T., Campopiano, D., Nikolova, P.V., Barran, P.E.: Insights into the conformations of three structurally diverse proteins: cytochrome c, p53, and MDM2, provided by variable-temperature ion mobility mass spectrometry. *Anal. Chem.* **87**, 3231–3238 (2015)
71. Larriba, C., Hogan, C.J.: Ion mobilities in diatomic gases: measurement versus prediction with non-specular scattering models. *J. Phys. Chem. A.* **117**, 3887–3901 (2013)
72. Larriba, C., Hogan, C.J.: Free molecular collision cross section calculation methods for nanoparticles and complex ions with energy accommodation. *J. Comput. Phys.* **251**, 344–336 (2013)
73. Wu, T., Derrick, J., Nahin, M., Chen, X., Larriba-Andaluz, C.: Optimization of long range potential interaction parameters in ion mobility spectrometry. *J. Chem. Phys.* **148**, 074102 (2018)